Design criterion for asymmetric twin-entry radial turbine for efficiency under steady and pulsating inlet conditions

Aolin Wang and Xinqian Zheng

Abstract

The internal combustion engine plays an important role in energy conservation and environmental protection. An efficient way to simultaneously reduce the engine fuel consumption and the emissions (NOx) is an asymmetric twin-entry turbine turbocharging system. The asymmetric twin-entry turbine uses a volute that has two scrolls in the axial direction with different throat areas. The smaller area scroll can increase the backpressure to support the exhaust gas recirculation system for lower NOx emissions; meanwhile, the larger area scroll can decrease the backpressure to reduce the exhaust resistance for lower fuel consumption. The area ratio is dependent on the required exhaust gas recirculation rate and fuel consumption. However, there are no guidelines for how to arrange the scrolls, and whether placing the big scroll on the hub side or the shroud side can provide improved results remains unknown. In this paper, two different design types are discussed for the asymmetric turbine, one with the big scroll on the hub side, while the other is on the shroud side. Also, the unsteady computational fluid dynamics (CFD) simulation is under steady and pulsating inlet conditions. The results show that when under steady inlet conditions, the efficiency of the asymmetric turbine with the big scroll on the shroud side is nearly 1.6% higher. However, when facing pulsating inlet conditions, the efficiency of the asymmetric turbine with the big scroll on the hub side is almost 1.1% higher. The difference is due to the different mass flow storage capacities of the two scrolls under pulsating inlet conditions. The design criterion for asymmetric twin-entry turbine states that if the turbocharger is designed for a large volume exhaust manifold, it is better to place the big scroll on the shroud side. If for a small volume exhaust manifold, it is better to set the big scroll on the hub side.

Keywords

Asymmetric turbine, twin-entry volute, efficiency, steady and pulsating, exhaust gas recirculation

Introduction

Turbocharger system has been an essential part of diesel engine due to its ability to increase power output and engine efficiency, and exhaust gas recirculation (EGR) system has been an efficient way to decrease the NOx emission of diesel engine.[1] Lapuerta et al.[2] evaluated a diesel engine NOx emission and found that EGR system together with turbocharger system can reduce the emission effectively. Zamboni et al.[3] got the similar conclusion and found that the turbocharger system helped the engine reach better fuel consumption. Figure 1 shows an exhaust system of a diesel engine, including EGR and turbocharger system. The EGR system takes part of exhaust gas from turbine inlet to compressor outlet, depressing the oxygen concentration of the inlet air to cut down the production of NOx.

Therefore, the back-pressure of EGR inlet (also turbine inlet) is required to be high enough to prevent backflow from EGR out (also the compressor outlet). As for turbocharger system, especially the turbine part, it is known that the back-pressure of turbine inlet is related to the inlet throat area[4] and the higher pressure requires smaller throat area, while the decrease of throat area will enhance the flow resistance and worse the engine scavenging process.[5] Based on this, turbine requires big

Turbomachinery Laboratory, State Key Laboratory of Automotive Safety and Energy, Tsinghua University, Beijing, China

Corresponding author:
Xinqian Zheng, Turbomachinery Laboratory, State Key Laboratory of Automotive Safety and Energy, Tsinghua University, Beijing 100084, China.
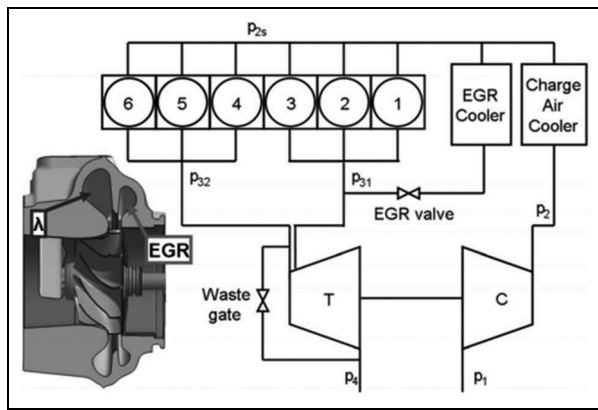Email: zhengxq@tsinghua.edu.cn

Figure 1. EGR and turbocharger system on diesel engine.[8]
EGR: exhaust gas recirculation.

throat area to reduce back-pressure, and this is opposite to the requirement of EGR system; neither the traditional single-entry turbine nor the symmetric twin-entry turbine can meet their demand at the same time. However, the asymmetric twin-entry turbine can make it, as shown in Figure 1; this kind of turbine has two scrolls with two different throat areas: the larger one provides sufficient flow capacity for power output, and the smaller one can increase the back-pressure for high enough EGR rate. Zhu and Zheng[6] studied the asymmetric twin scroll turbocharging system and found it can improve the engine efficiency and emission performance. Schmidt et al.[7] named the two different scrolls as "EGR scroll" for the smaller and "Lambda scroll" for the larger to represent their different functions.

Since the two scrolls are designed asymmetrically in the axial direction, it is interesting to think about the effect it may have on turbine performance. We know that the impeller of a turbine is also asymmetric in the axial direction, and the shroud side has a more significant curvature than hub side; is this feature has any effect on turbine efficiency or flow field? Unfortunately, it remains unclear nowadays. Based on this, it is important to address which arrangement of scrolls, the big scroll on the impeller hub side or the shroud side, can provide better efficiency. Currently, the most popular kind of asymmetric twin-entry turbine places the big scroll on the shroud side, as shown in Figure 1. This type of arrangement is based on a list of previous studies. Dale and Watson[9] measured a symmetric twin-entry turbine's performance over a wide range of steady partial inlet conditions. They found that for the symmetric twin-entry turbine, the peak efficiency point occurred when the scroll at the impeller shroud side has more mass flow than the hub side scroll, instead of the full inlet condition. However, the authors did not explain this phenomenon. Baines and colleagues[10–12] found the same phenomenon whereby the flow preferred to enter the impeller from the shroud side. They performed experiments and measured the performance and the flow field of a twin-entry radial turbine under steady full and partial inlet conditions. And they

hypothesized that the impeller hub side leading edge is more sensitive to positive incidence angle and this may cause a penalty for efficiency. Still, no experimental evidence can support the hypothesis. Based on the conclusion above, the asymmetric twin-entry turbine is mainly designed with the big scroll on the shroud side. Therefore, the more mass flow goes into impeller in the high-efficiency region, and this can provide high performance. Muäller et al.[13] give the same explanation for their asymmetric twin-entry turbine on a Benz 11-L diesel engine. Brinkert et al.[8] also used the same asymmetric model to represent the asymmetric twin-entry turbine.

However, the research works above are based only on steady inlet conditions, without any further investigation under pulsating inlet conditions. Since the twin-entry turbocharger is wildly used on gasoline engines which almost adopt the pulsating turbocharging system to decrease the turbine lag, it is essential to investigate the turbine performance under pulsating inlet conditions to make clear whether it keeps the same as or differ from the steady inlet conditions. Quasi-steady assumption is one of the available methods to analyze turbine pulsating performance; if the turbine operation were quasi-steady, the pulsating flow results would follow the steady-flow curve, that is to say, if the quasi-steady assumption is satisfied, the turbine performance keeps the same under steady and pulsating inlet conditions. However, research works of Wallace and colleagues[14–16] and Woods and Norbury[17] reported that the quasi-steady assumption tends to be unsatisfactory when pulsating frequency increases. Dale and Watson[9] tested the pulsating turbine performance on a test rig, and their results showed a noticeable deviation from the steady-flow curve, demonstrating the inadequacy of the quasi-steady assumption. The more recent investigations on the unsteady performance of twin-entry turbines were given by Galindo et al.;[18] they used the CFD method to simulate the flow characteristics of a radial turbine in pulsating flow and found that the primary source of non-quasi-steadiness of the turbine is the turbine volute. If the turbine volute has greater length and volume, the degree of non-quasi-steadiness becomes severe. Other work also focused on the quasi-steady assumption such as the research work in Martinez-Botas and colleagues.[19–21] Based on these studies, De Bellis et al.[22] carried out one-dimensional (1D) simulation and experiment to analyze turbine performance under steady and unsteady conditions and found that under a pulsating flow, the turbine rotor can be seen as a steady state while the volute showed storage effects within it. The flow in the volute is influenced by unsteady effects of pulsating inlet, and the flow field at the rotor inlet is affected, which may lead to a change in turbine efficiency.

Therefore, compared with under steady inlet conditions, the performance of the turbine is quite different when under pulsating inlet conditions, and it is the volute that causes the difference. Due to this, the

popular type of asymmetric turbine shown in Figure 1 may not be suitable for pulsating turbocharger system, so it is important to investigate the effect of the asymmetric volute on turbine performance and find out which type of arrangement can better suit pulsating inlet conditions. Unfortunately, there is relatively less research on asymmetric turbine under pulsating inlet condition and even rare study on another type of asymmetric volute that places the small scroll on the shroud side.

In the present paper, the authors compared the performance and flow field of two different types of asymmetric turbines together with another symmetric turbine under steady and pulsating inlet conditions. Based on the different performances of the three turbines under different inlet conditions, a brief explanation is given and a design criterion for the asymmetric twin-entry turbine when under steady or pulsating inlet conditions is described.

Test facility

The turbine dynamometer test rig, on which the turbine can be tested in isolation from the rest of the turbocharger, is shown in Figure 2. There are four pressure sensors at the turbine inlet, the arrangement is equispaced at the circumferential direction and the measurement precision is 0.04%. The number of inlet temperature sensors is 3 and they have the same arrangement; the precision is 0.25°C. At the turbine outlet, the arrangement of the pressure sensors is same as inlet condition, but there is only one temperature sensor. The hydraulic dynamometer is used to absorb the power output, and the formula to calculate the turbine efficiency η_t is as follows

$$\eta_t = \frac{P_t}{m_f \times C_p \times \Delta T_0} \tag{1}$$

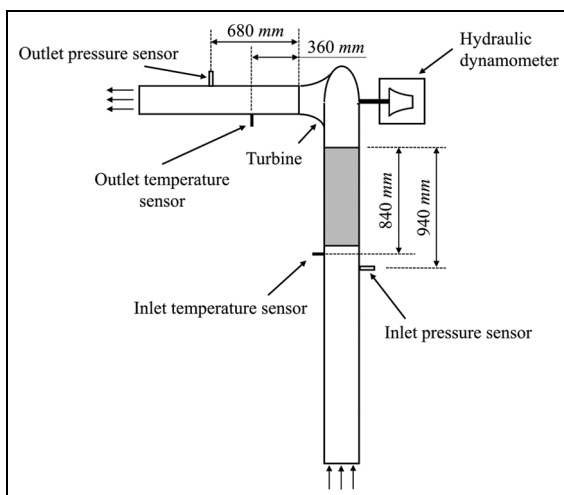where P_t is the turbine output power that is tested by dynamometer and m_f is mass flow rate; ΔT_0 is the

difference between the total temperature of the inlet T_{01} and the outlet T_{03}.

For further explanation, the parameter that the dynamometer can measure directly is the torque, so P_t is defined as follows

$$P_t = \frac{T_q \times n}{9550} \tag{2}$$

where T_q is the torque, and n is the rotational speed. What's more, considering the inaccuracy of the temperature measurement caused by the uniformity of the turbine outlet condition, the value of the outlet total temperature T_{03} is calculated as follows

$$T_{03} = \frac{T_{01}}{\left(\frac{P_{01}}{P_{03}}\right)^{\frac{\gamma}{\gamma-1}}} \tag{3}$$

where P_{01} and P_{03} are the inlet and outlet total pressures, respectively. As the static inlet temperature of the test rig is controlled under 40°C, heat exchange with the ambient environment can be neglected, and the flow can be considered as isentropic.

Numerical methodology

Numerical model

There are three types of models used to analyze the symmetric and asymmetric twin-entry scroll turbines. The turbine geometry models, which are shown in Figure 3, consist of the volute and the impeller. The detailed parameters of the geometry are shown in Table 1. The three models use the same impeller but are combined with different volutes. The asymmetric design refers to that where the throat area of the volute shroud side scroll is bigger than that of the hub side, and the asymmetric OP is the model with the opposite features as the asymmetric design. The total throat area of these three models remains the same, and they also have the same volute cross-sectional area distribution feature to ensure a similar flow capacity.

The prototype of the asymmetric turbine is a commercial turbine installed at a 11-L inline six-cylinder diesel engine. The six cylinders are connected in two groups of three, and each group feeds one inlet of the
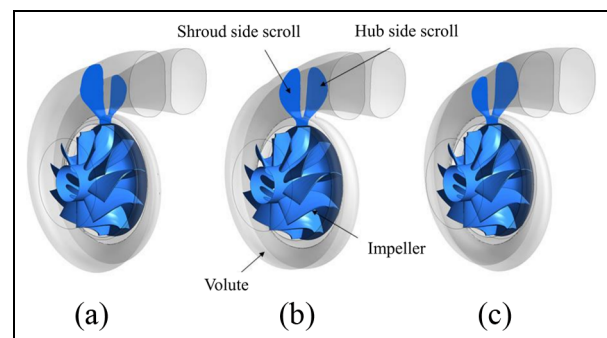

Figure 2. Sketch map of the test bench.

Figure 3. Turbine geometry models: (a) asymmetric, (b) symmetric and (c) asymmetric OP.

Table 1. Turbine geometric parameters.

Parameter	Value
Blade numbers	10
Volute outlet radius	42.80 mm
Volute outlet width	11.38 mm
Impeller inlet radius	41.75 mm
Impeller outlet radius	27.66 mm
Tip clearance	0.45 mm
Inlet blade angle	0°
Throat area	1168 mm^2
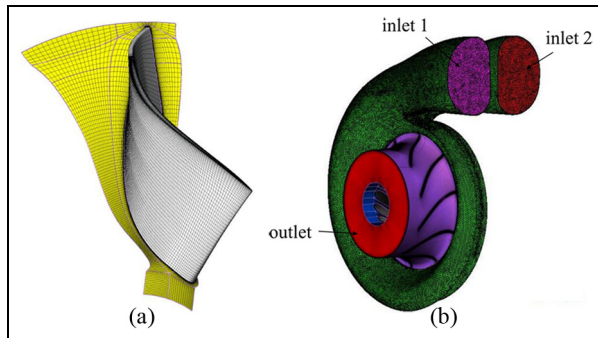
Figure 4. Single passage of the impeller mesh (a) and the domain and boundaries (b).

Figure 5. The grid size independence validation.

twin-entry turbine. This paper focuses on the different performance of the asymmetric and asymmetric OP turbine; the symmetric type works as a reference.
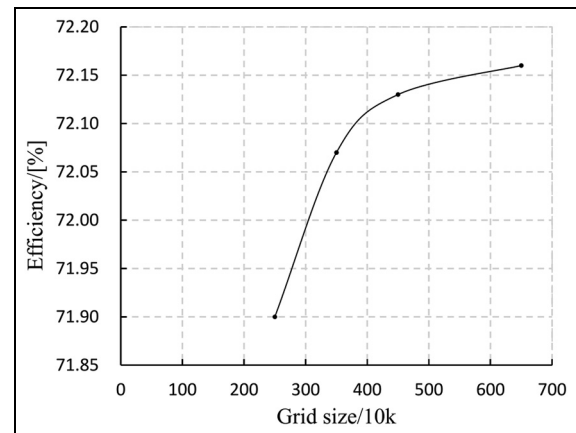
Considering the nonuniform circumferential flow field caused by the volute at the impeller inlet, it is necessary to simulate the entire impeller flow domain, as opposed to the single passage domain. The mesh of the impeller and volute are shown in Figure 4. The structured mesh is used for the impeller with a total of 4,360,760 grids points. The computational domain of the volute adopted the unstructured mesh with a total of 2,037,995 grids points. Therefore, the total grid number of the model is more than 6 million.

Numerical method

The simulation was conducted with the ANSYS CFX solver, which is based on the three-dimensional compressible finite volume scheme to solve steady-state Reynolds-averaged Navier–Stokes equations with the conservative formulation. Considering the calculation cost and time, the k–ε turbulence model is selected and can accurately simulate the flow separation and vortices. The validation of the mesh independence is shown in Figure 5, and as seen, 5 or 6 million grids points can provide reasonably accurate numerical results.

Simulation procedure

The absolute total pressure and total temperature are imposed as the inlet boundary conditions, the absolute

static pressure is imposed as the outlet boundary condition and the data are derived from the experimental measurements. Inlet1 and inlet2 employ the boundary conditions separately to make different inlet conditions for each scroll when under the pulsating inflow condition. At solid boundaries, as the turbine test rig adopts the cold inlet air and there is heat insulator outside the pipe, adiabatic wall conditions are imposed for the simulation, which means no slip and no heat transfer. The frozen rotor model is imposed at the interface.

Simulation validation

The results comparing the simulated total-to-static isentropic efficiency and the mass flow rate under full admission conditions with the experiments are shown in Figure 6. The simulated efficiency is defined as follows

$$\eta_{ts} = \frac{T_{01} - T_{03}}{T_{01}\left[1 - \left(\frac{P_3}{P_{01}}\right)^{(\gamma-1)/\gamma}\right]} \qquad (4)$$

where T_{01} and T_{03} are the inlet and outlet total temperatures, respectively. P_3 and P_{01} are the static outlet pressure and total inlet pressure, respectively.

The experiments concern the asymmetric turbine (a), and the four lines refer to the rotational speed 64,000, 80,000, 96,000 and 112,000 r/min, respectively (Figure 3). The results indicate that the simulation is in reasonable agreement with the experimental data both for the efficiency and for the flow capacity with a maximum discrepancy of 0.9%. The noticeable differences are toward the lower speed and lower expansion ratio range of the efficiency. This may be a result of the experiment deviation because it is difficult to maintain the test speed at the required value at lower rotating speeds and the deviation would be more significant than at higher rotating speeds. The good agreement of the flow capacity can also prove the conclusion because the test of the mass flow rate is negligibly affected by the change in speed.
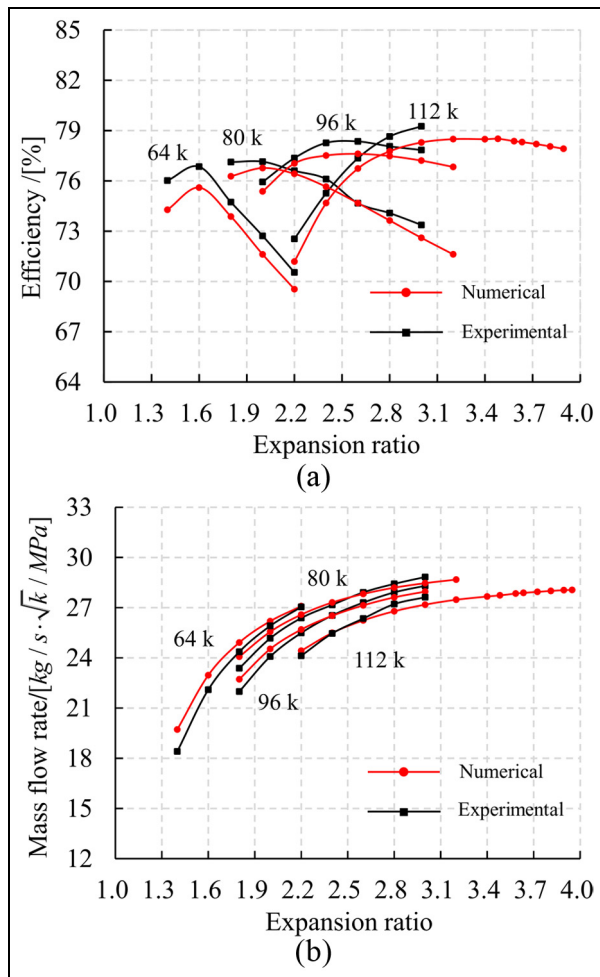
Figure 6. Performance comparison between the numerical and experimental results: (a) efficiency and (b) mass flow rate.

Figure 7. Performance comparison between the symmetric and the two different asymmetric turbines: (a) efficiency and (b) mass flow rate.

The CFD results and experiment data can match well with each other under steady inlet conditions, and experiments under pulsating inlet conditions will be carried out in the future to fine down the validation of the numerical model.

In this paper, first, the performance and flow fields of the three types of turbines are compared under steady inlet conditions to determine the mechanism of the efficiency change and the geometric effects on the turbine performance. Then, the performance and flow fields under pulsating inlet conditions are investigated to discover the pulse effects. Finally, based on the results and analysis, a criterion is established for the asymmetric twin-entry turbine design under steady and pulsating inlet conditions.

Results under steady equal inlet conditions

The numerical results of the three simulated models are shown in Figure 7. The volute throat area was designed to maintain the same flow capacity in the three models, as shown in the mass flow rate map. It can be seen that at low speeds, the mass flow rates of the three turbine
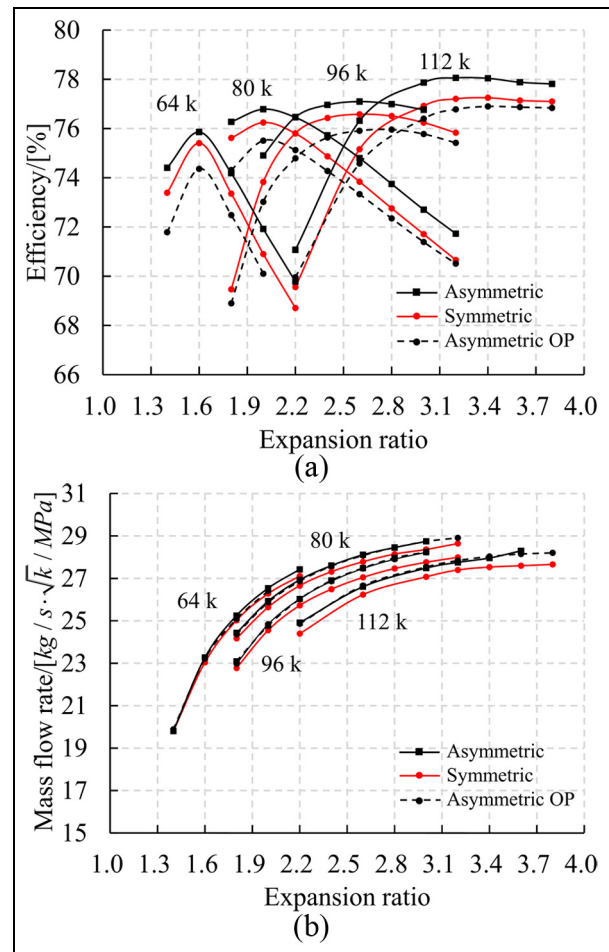
types are nearly the same, but at the highest speed, there was a drop in the mass flow rate of approximately 0.2%, which may cause a drop in the efficiency of the symmetric turbine at high speeds, putting it close to the asymmetric OP model. Over the entire range of working conditions, the asymmetric turbine has the best turbine efficiency, while the OP has the worst, with the symmetric turbine in the middle. What is interesting is that the efficiency drops between these three models at intervals of approximately 0.8%. Based on this finding, we take the speed line 96,000 r/min condition for further investigation to simplify the research process.

Figure 8 shows the turbine and component performance comparison results. It can be seen that the flow loss in the volute remains nearly constant with the expansion ratio, while the rotor efficiency shows the same trend as turbine efficiency. Although the symmetric turbine has the lowest total pressure loss coefficient, this contributes little to the turbine performance, and considering that the test data used for the calculations are measured at the interface, the mixing flow at the volute outlet domain may contribute to the rise in the asymmetric and OP's loss coefficients. It is clear
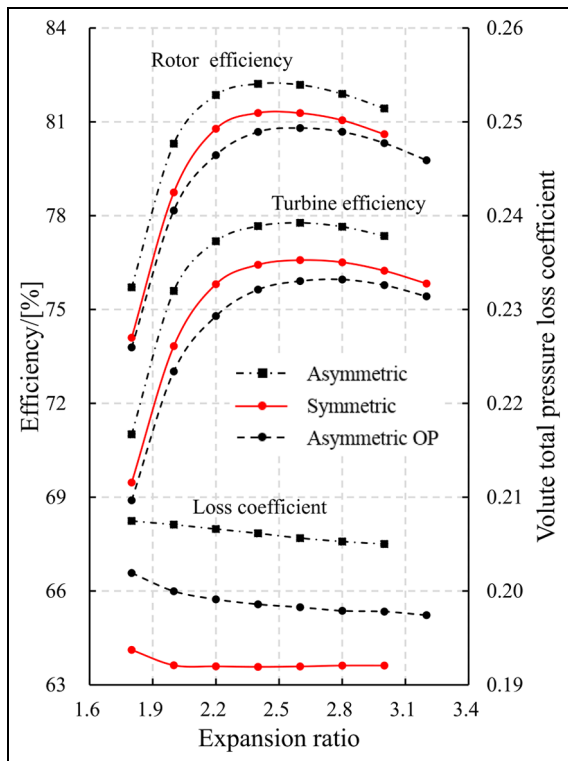
Figure 8. Turbine and component performance.

Figure 9. Rotor efficiency and radial velocity distribution at the impeller leading edge.

that the turbine efficiency is mainly determined by the rotor efficiency and that the flow loss in the volute has a negligible effect. The main function of the volute is to provide the rotor inlet flow field, which may affect the rotor efficiency. Therefore, even if the volute has different geometries, the key point to determine the turbine efficiency is the flow field at the impeller inlet position.

Figure 9 shows the shroud to hub spanwise distribution for the rotor efficiency and radial velocity at the impeller leading edge. The rotor efficiency distribution is a hypothetical value that signifies the specific power output that a unit mass of gas can provide if it enters the impeller at a given spanwise position. The values are calculated along the spanwise direction, at the leading edge and the corresponding trailing edge. The radial velocity represents the inlet mass flow, and the rotor efficiency distribution and the match with the mass flow distribution determine the impeller efficiency. Thus, if the high radial velocity position matches well with the high-efficiency region, a senior rotor efficiency is achieved.

In Figure 9, the efficiency is higher at the hub side than at the shroud side, and the asymmetric case has the highest efficiency, while the OP has the lowest. For the mass flow distribution for the asymmetric case, symmetric case and OP case, the maximum mass flow position moves from the hub side to the shroud side, or from the high-efficiency region to the low-efficiency region. These two reasons can explain the differences in the rotor efficiency.

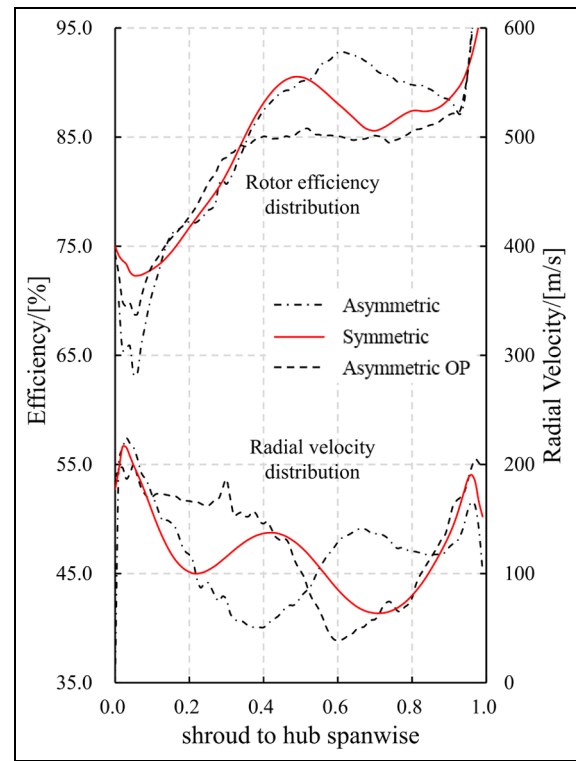Figure 10 shows the rotor inlet incidence angle of the three turbine models along the plane at 0.01 mm

upstream of the rotor leading edge, which is the critical parameter to evaluate the rotor performance. It is recognized that optimum incidence is in the region of $-20°$ to $-40°$ and that a deviation from this region can cause a drop in the efficiency. Moustapha et al.[23] concluded that the radial turbine rotors are much more sensitive to positive incidence than to extremes of negative incidence. Then, Baines[24] put forward a postulate that the rotor is more sensitive to the positive incidence near the hub surface to explain the difference in the efficiencies under the hub and shroud side partial admission condition. Nevertheless, he did not show any experimental or CFD results to support the postulate.

It can be seen from Figure 10 that the positive incidence appears in the region that corresponds to the position of the large volute scroll. From Figure 10(a) to (c), the positive incidence region moves from the shroud side to the hub side of the impeller, causing the efficiency to decrease. These results correspond to Baines' hypothesis.

From the flow field at the rotor inlet region shown in Figure 11, a vortex exists caused by the flow separation at the hub side near the suction surface of the impeller. Compared to the static entropy distribution, it can be seen that there are two high entropy regions in the flow channel, one of which is near the hub and corresponds to the vortex. The other is near the shroud, which is caused by the tip clearance flow. Also, the entropy gain caused by the vortex is larger than the tip clearance entropy gains.
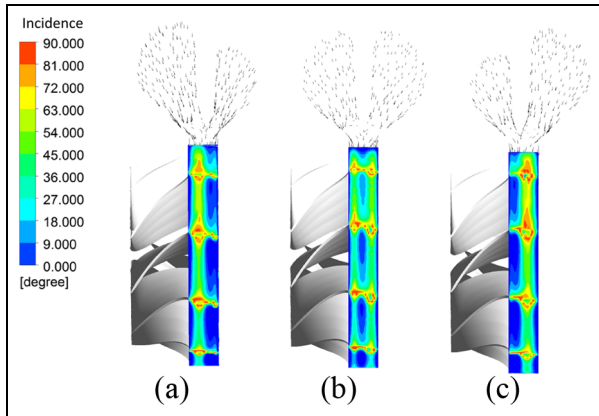
Figure 10. Incidence angle distribution at the impeller leading edge: (a) asymmetric, (b) symmetric and (c) asymmetric OP.
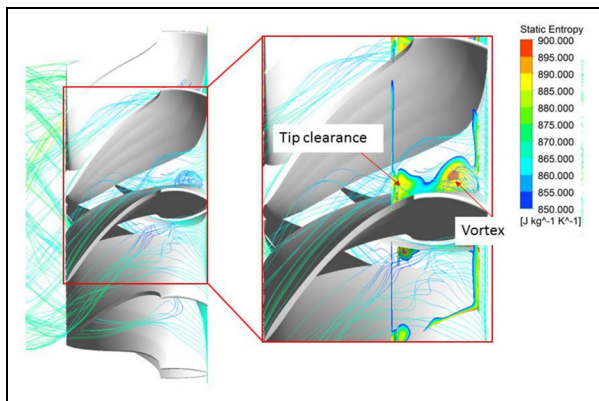

Figure 11. Flow field and static entropy at the impeller inlet region.

Moreover, the vortex region is also where the high static entropy appears. It is well known that a negative

incidence angle can weaken the flow separation, while a positive angle can aggravate it. Therefore, when the large volute scroll is placed on the shroud side, the negative incidence region is at the hub side of the impeller. This can weaken the flow separation, fade or even erase the vortex, which may improve the turbine performance. When the larger volute scroll is placed on the hub side, the positive incidence region is at the hub side, which may enhance the degree of the flow separation and the vortex could become severe, leading to the drop in efficiency. This is illustrated in the flow field in Figure 12.

The static entropy distribution from Figure 13 at the vortex region shows the same conclusion. It can be seen that the asymmetric case only has an entropy gain caused by tip clearance, while the asymmetric OP model has the most severe entropy gain at the vortex region. This can explain the efficiency differences between these three models.

Figure 14 shows the velocity distribution at the volute outlet plane at the impeller trailing edge. It illustrates that these three models have nearly the same outlet flow field, and their mean velocities are 140.3, 141.2 and 142.1 m/s, respectively. This means that the efficiency differences of the impellers are mainly caused by the difference in the inlet flow condition.

Results under the pulsating inlet condition

When the engine adopted the pulsating turbocharger system, the exhaust pressure is a pulse wave with a specific amplitude and a specific main frequency, and the frequency is connected with the engine speed. We can use an ideal sinusoidal signal to represent the real engine exhaust pressure pulse wave as the turbine pulsating inlet condition. This paper has simplified the
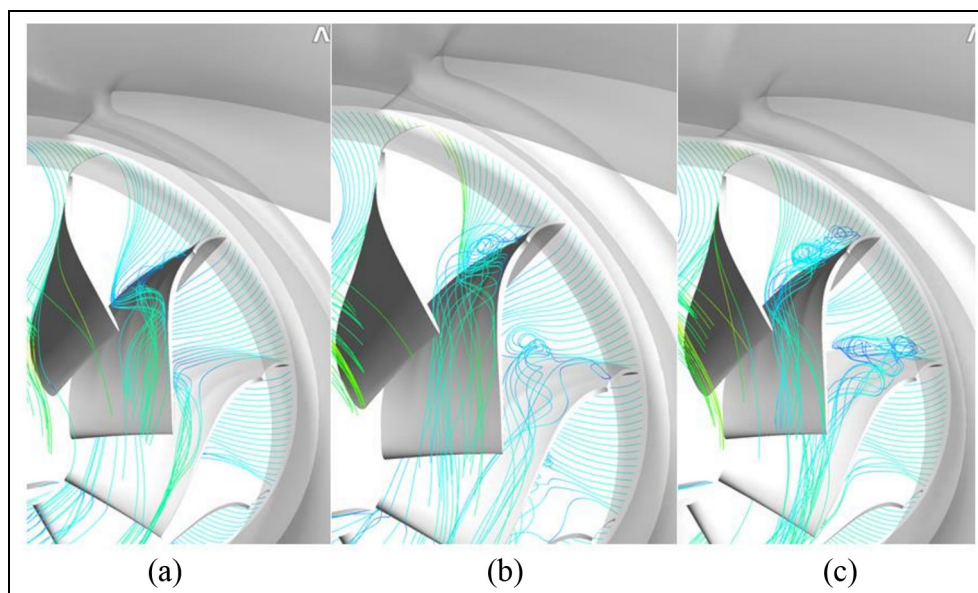

Figure 12. Flow field in the rotor passage: (a) asymmetric, (b) symmetric and (c) asymmetric OP.
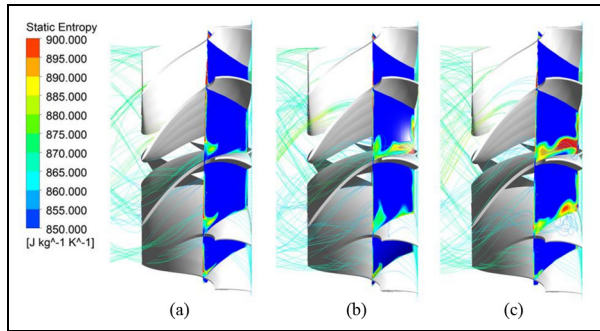
Figure 13. Static entropy distribution in the rotor passage: (a) asymmetric, (b) symmetric and (c) asymmetric OP.

pulsating inlet condition to a sinusoidal signal while kept the amplitude and frequency similar to the engine real exhaust pressure, and the prototype pressure wave is from a six-cylinder diesel engine in Muäller et al.[13]

The pulsating frequency of the simulation is 25 Hz, corresponding to the power output condition for this 11-L diesel engines. This working point demand is more stringent to fuel consumption, which means that a high turbine efficiency is required. During pulsating inlet conditions, the volute shroud side scroll and the hub side scroll face two different inlet pulses that have a reverse phase as shown in Figure 15. Considering the two isolation inlet conditions of the volute, the isentropic efficiency of the turbine at a specific time is defined as follows

$$\eta = \frac{m_{1s} + m_{1h} - (m_{1s} + m_{1h}) \cdot T_{03}/T_{01}}{m_{1s}\left(1 - (P_3/P_{01s})^{\frac{\gamma-1}{\gamma}}\right) + m_{1h}\left(1 - (P_3/P_{01h})^{\frac{\gamma-1}{\gamma}}\right)} \tag{5}$$

Then, the volute total pressure loss coefficient is newly defined as follows

$$K = \frac{m_{1s}P_{01s} + m_{1h}P_{01h} - (m_{1s} + m_{1h})P_{02}}{(m_{1s} + m_{1h})(P_{02} - P_2)} \tag{6}$$

As for rotor efficiency, considering that the form of the inlet and outlet remains the same as in the steady situation, the calculation remains unchanged.

Figure 15 shows the performance of these three turbines under a 25-Hz pulsating inlet flow condition. The

time-averaged efficiencies for these three turbines are 74.48%, 74.69% and 75.54%, corresponding to the asymmetric, symmetric and asymmetric OP model, respectively. The asymmetric type has the worst performance, which is a contrary result of the steady performance where the asymmetric turbine shows the best performance. This means that the performances of the turbines are different when under steady and pulsating inlet flow conditions.

Under the pulsating inlet conditions, the highest efficiency points appear for all three models when the hub and shroud inlet pressures are equal. The efficiency drops when facing the partial admission condition, especially in the situation when the hub side inlet has the highest back-pressure.

When the volute hub side inlet has the lower pressure, corresponding to less mass flow, the efficiencies of these three models are nearly the same, and the asymmetric turbine is improved over the other two. However, when the hub side has more pressure, the efficiency drops and the asymmetric turbine is affected the most, causing a decrease in the average efficiency. Therefore, the inlet condition at the volute hub side is the main factor to control the twin-entry turbine performance, and the decrease in the mass flow may not cause a noticeable rise in the efficiency, but the increase in mass flow will lead to an efficiency drop. If the twin-entry turbine is symmetric, the high efficiency appears when the shroud side inlet mass flow rate is larger than the hub side and drops when the mass flow is less, which agrees with previous conclusions under steady inlet conditions from the literature.

The asymmetric model that places the small scroll on the hub side is affected more by the hub side inlet, and the OP model that places the big scroll on the hub side is affected less. Therefore, the small scroll has more influence on the turbine performance. In summary, the small scroll on the hub side is the main cause of determining the turbine performance, especially the efficiency drop when facing partial admission conditions.

Comparing the component performance shown in Figure 16 with the turbine efficiency, the same conclusion as the steady-state condition was found, whereby the turbine performances are mainly determined by the
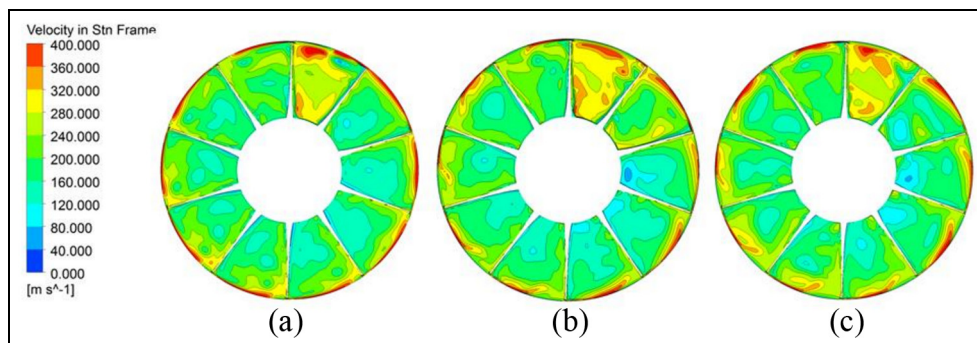

Figure 14. Exit flow field at the impeller trailing edge: (a) asymmetric, (b) symmetric and (c) asymmetric OP.
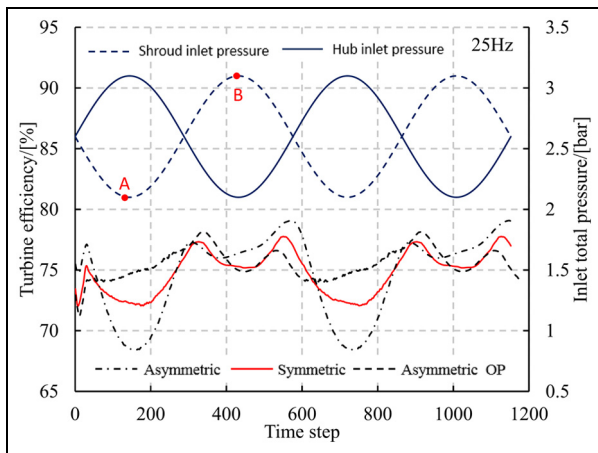
Figure 15. Turbine performance under the 25-Hz pulsating inlet condition.
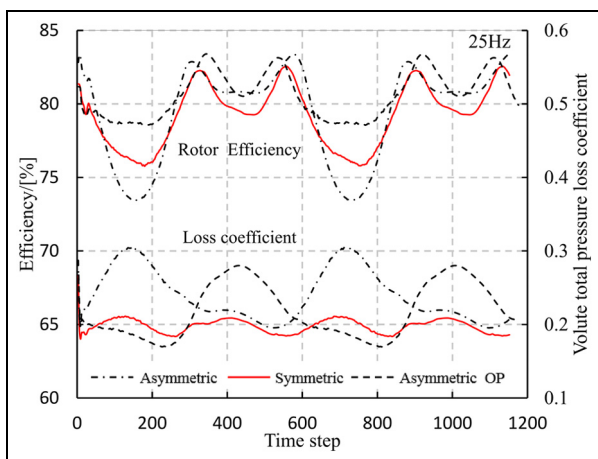

Figure 16. Component performance under the 25-Hz pulsating inlet condition.

rotor performance and the contribution of the flow loss in the volute is marginally negligible.

Figure 17 shows the rotor efficiency and the radial velocity distribution at the impeller leading edge at time steps A and B. Time step A corresponds to the extreme partial admission condition when all of the turbines have the efficiency drop. It can be seen that the radial velocity distribution is almost the same for the three models at this time. The most important factor is the efficiency distribution, and it is clear that the OP model has the highest efficiency and that the asymmetric one has the lowest, which influences the turbine performance.

Similar to the results under steady conditions, the efficiency distribution for the pulsating inlet condition is affected by the incidence angle at the impeller inlet position, especially in the positive incidence region. Figure 18 illustrates that from the asymmetric case to the OP case, the positive incidence region moves from the hub side to the shroud side. As mentioned before, the positive incidence angle can sever the vortex in the

impeller flow path and cause the efficiency to drop. The impeller hub side leading edge is more sensitive to a positive incidence angle than the shroud side. Therefore, as the positive incidence region moves from the hub to the shroud side, the efficiency recovers, which can explain the performance difference in these three models.

Under equal steady inlet conditions, the mass flow in the big scroll is larger than in the small scroll, resulting in a faster flow velocity and positive incidence angle. Combined with the conclusion that the hub side of the impeller is more sensitive to positive incidence, if the big scroll is on the hub side, the efficiency drops. Under pulsating inlet conditions, the efficiency is different to the steady-state situation, especially for the asymmetric turbine when the hub side is charged more than the shroud side. This is because the big volute has a higher mass flow storage ability than the small one, that is, the small scroll response is more sensitive to the pressure rise and flow in the small scroll is accelerated, leading to a higher outlet velocity, which causes a greater incidence angle. When the pressure rises for the asymmetric turbine with the small scroll on the hub side, a positive incidence angle region occurs at the hub side and the efficiency drops.

Conclusion

Simulations for a symmetric and two opposite asymmetric twin scroll turbines under steady and pulsating inlet conditions have been conducted to study the differences in the flow field and performance between these three types of turbines; an experiment was carried out to validate the numerical methodology under steady inlet conditions, and the conclusions are as follows:

1. Under steady admission conditions, the asymmetric turbine with the big scroll on the shroud side has the best efficiency, which is nearly 1.6% higher than the contrary type (OP). Under steady full inlet conditions, the incidence angle at the region outside the big scroll is positive. The impeller hub side leading edge is more sensitive to the positive incidence than the shroud side due to the hub side vortex in the impeller flow path, while the positive incidence severs the vortex and causes the efficiency to drop. Therefore, if the big scroll is on the hub side, the efficiency is worse than on the shroud side.

2. Under pulsating inlet conditions, the results are contrary to the steady state. The asymmetric turbine with the big scroll on the hub side (OP) has the best efficiency, which is nearly 1.1% higher than on the shroud side. Since the small scroll mass flow capacity is smaller than the big scroll, when the backpressure increases, the flow in the small scroll is faster than in the big scroll, which may cause a positive incidence angle at the impeller
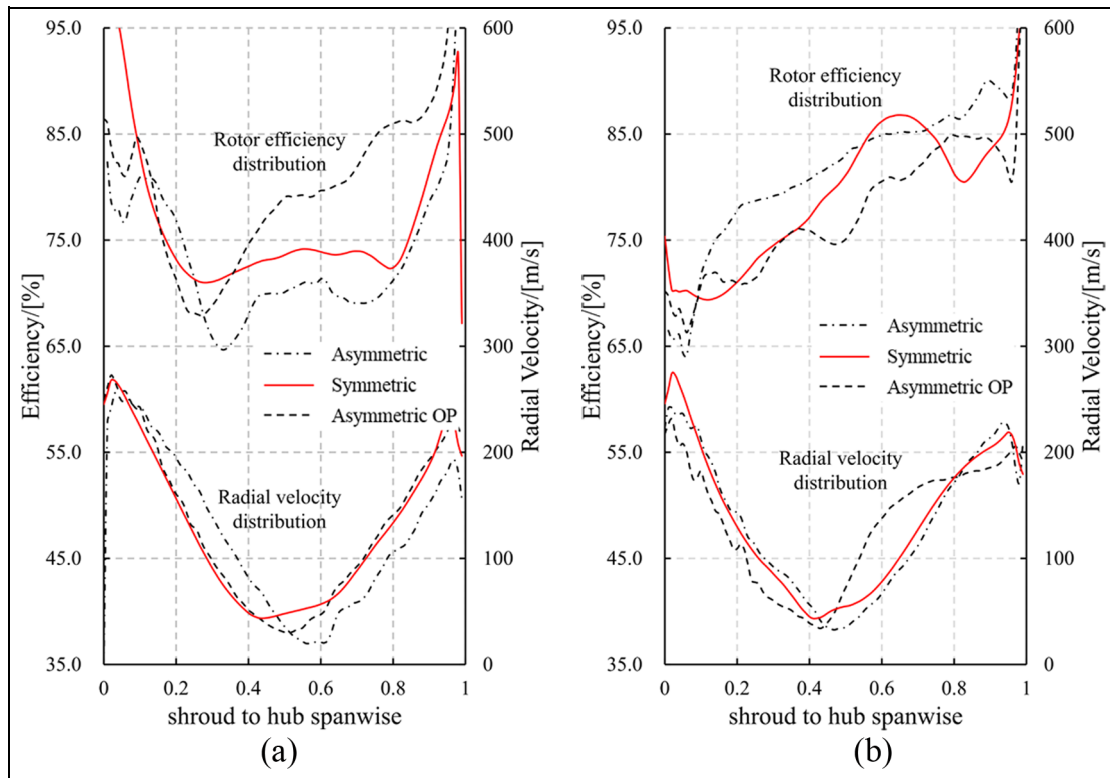
Figure 17. Rotor efficiency and radial velocity distribution at the impeller leading edge: (a) A time step and (b) B time step.
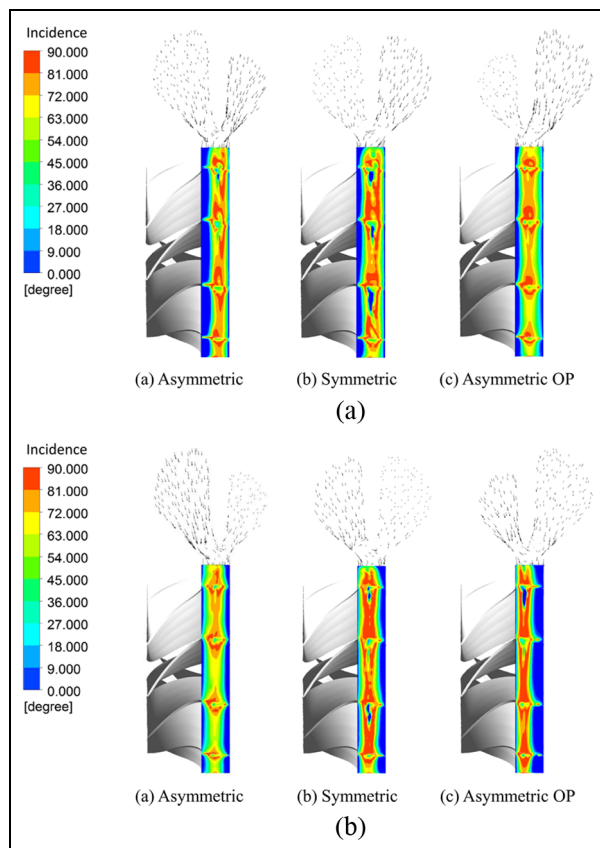

Figure 18. Incidence angle distribution at the impeller leading edge: (a) A time step and (b) B time step.

leading edge. Therefore, if the small scroll is set on the hub side, the positive incidence appears at the hub side and the efficiency is degraded.

3. The design criterion for the asymmetric twin-entry turbine state is as follows: when under steady inlet conditions (e.g. constant-pressure turbocharging system on the diesel engine), it is better to place the big scroll on the shroud side. When under pulsating inlet conditions (e.g. pulse turbocharging system on the gasoline engine), it is better to place the big scroll on the hub side.

4. Simulation calculations were conducted for a given rotational speed and a given simplified scroll input pressure. It must be controlled whether these conclusions remain the same for real engine pressure conditions and other engines speeds. Experiments will have to be carried out to check these results.

Declaration of conflicting interests

The author(s) declared no potential conflicts of interest with respect to the research, authorship and/or publication of this article.

Funding

The author(s) received no financial support for the research, authorship and/or publication of this article.

References

1. Dürnholz M, Eifler G and Endres H. Exhaust-gas recirculation: a measure to reduce exhaust emissions of DI diesel engines, SAE technical paper 920725, 1992.
2. Lapuerta M, Hernandez JJ and Gimenez F. Evaluation of exhaust gas recirculation as a technique for reducing diesel engine NO$_X$ emissions. *Proc IMechE, Part D: J Automobile Engineering* 2000; 214: 85–93.
3. Zamboni G, Moggia S and Capobianco M. Hybrid EGR and turbocharging systems control for low NO$_X$ and fuel consumption in an automotive diesel engine. *Appl Energ* 2016; 165: 839–848.
4. Moustapha H, Zelesky MF, Baines NC, et al. *Axial and radial turbines*, vol. 2. White River Junction, VT: Concepts NREC, 2003.
5. Wijetunge RS, Hawley JG and Vaughan ND. An exhaust pressure control strategy for a diesel engine. *Proc IMechE, Part D: J Automobile Engineering* 2004; 218: 449–464.
6. Zhu D and Zheng X. Asymmetric twin-scroll turbocharging in diesel engines for energy and emission improvement. *Energy* 2017; 141: 702–714.
7. Schmidt S, Rose MG, Müller M, et al. Variable asymmetric turbine for heavy duty truck engines. In: *ASME turbo expo 2013: turbine technical conference and exposition*, San Antonio, TX, 3–7 June 2013, pp.V05AT23A013-1–V05AT23A013-11. New York: ASME.
8. Brinkert N, Sumser S, Weber S, et al. Understanding the twin scroll turbine: flow similarity. *J Turbomach* 2013; 135: 021039.
9. Dale A and Watson N. Vaneless radial turbocharger turbine performance. In *Proceedings of the Institution of Mechanical Engineers, 3rd International Conference on Turbocharging and Turbochargers*, London, May 6–8 1986, Paper No. C110/86, pp. 65–76. Mechanical Engineering Publications.
10. Baines NC and Lavy M. Flows in vaned and vaneless stators of radial inflow turbocharger turbines. In: *IMechE turbocharging and turbochargers conference*, London, May, Paper No. C405/005, pp. 7–12, Mechanical Engineering Publications.
11. Baines NC and Yeo JH. Flow in a radial turbine under equal and partial admission conditions. In: *IMechE European conference on turbomachinery: latest developments in a changing scene*. London, March 12–13, Mechanical Engineering Publications, Paper No. C423/002, pp. 103–112.
12. Baines NC, Hajilouy-Benisi A and Yeo JH. The pulse flow performance and modelling of radial inflow turbines. In: *IMechE conference publications*, 1994; 6: 209–220. London: Medical Engineering Publications.
13. Muäller M, Streule T, Sumser S, et al. The asymmetric twin scroll turbine for exhaust gas turbochargers. In: *ASME turbo expo 2008: power for land, sea, and air*, Berlin, 9–13 June 2008, pp.1547–1554. New York: ASME.
14. Wallace FJ and Blair GP. The pulsating-flow performance of inward radial-flow turbines. In: *ASME 1965 gas turbine conference and products show*, Washington, DC, 28 February–4 March 1965. New York: ASME.
15. Wallace FJ, Cave PR and Miles J. Performance of inward radial flow turbines under steady flow conditions with special reference to high pressure ratios and partial admission. *Proc IMechE* 1969; 184: 1027–1042.
16. Wallace FJ and Miles J. Performance of inward radial flow turbines under unsteady flow conditions with full and partial admission. *Proc IMechE* 1970; 185: 1091–1105.
17. Woods WA and Norbury JF. Pulse flow performance of axial turbines for marine turbochargers. *In: ISME Tokyo*, 1973, Tokyo: The Marine Engineering Society of Japan. pp.1–5.
18. Galindo J, Fajardo P, Navarro R, et al. Characterization of a radial turbocharger turbine in pulsating flow by means of CFD and its application to engine modeling. *Appl Energ* 2013; 103: 116–127.
19. Costall AW, McDavid RM, Martinez-Botas RF, et al. Pulse performance modeling of a twin entry turbocharger turbine under full and unequal admission. *J Turbomach* 2011; 133: 021005.
20. Mamat AMB and Martinez-Botas RF. Mean line flow model of steady and pulsating flow of a mixed-flow turbine turbocharger. In: *ASME turbo expo 2010: power for land, sea, and air*, Glasgow, 14–18 June 2010, pp.2393–2404. New York: ASME.
21. Rajoo S, Romagnoli A and Martinez-Botas RF. Unsteady performance analysis of a twin-entry variable geometry turbocharger turbine. *Energy* 2012; 38: 176–189.
22. De Bellis V, Marelli S, Bozza F, et al. 1D simulation and experimental analysis of a turbocharger turbine for automotive engines under steady and unsteady flow conditions. *Energ Proced* 2014; 45: 909–918.
23. Moustapha SH, Kacker SC and Tremblay B. An improved incidence losses prediction method for turbine airfoils. In: *ASME international gas turbine and aeroengine congress and exposition*, Toronto, ON, Canada, 4–8 June 1989, pp.V001T01A100-1–V001T01A100-10. New York: ASME.
24. Baines, N. C. (1998). A meanline prediction method for radial turbine efficiency. In *Proceedings of the Institution of Mechanical Engineers, 6th International Conference on Turbocharging and Air Management Systems*, London, November 3–5, Mechanical Engineering Publications, Paper No. C554–6, pp. 315–325.

Appendix I

Notation

K	total pressure loss coefficient
m	mass flow rate (kg/s)
P	pressure (Pa)
T	temperature (K)
γ	heat ratio
η	efficiency

Subscripts

0	total parameter
1	volute inlet
2	volute outlet
3	impeller outlet
h	hub side
s	shroud side